

# Influence of deposition conditions on the thermal stability of ZnO:Al films grown by rf magnetron sputtering

F.-J. Haug, Zs. Geller, H. Zogg, and A. N. Tiwari<sup>a)</sup>

*Thin Film Physics Group, Laboratory for Solid State Physics, Swiss Federal Institute of Technology, Technoparkstrasse 1, 8005 Zürich, Switzerland*

C. Vignali

*Centro Interfacoltà Misure, University of Parma, Viale delle Scienze 23 A, 43100 Parma, Italy*

(Received 13 April 2000; accepted 2 October 2000)

The resistivity and the thermal stability of transparent conducting ZnO layers doped with aluminum have been correlated with the conditions of the sputtering process. Layers deposited at low rf power density ( $\sim 1.3$  to  $2.6$  W/cm<sup>2</sup>) exhibit a low resistivity of  $9 \times 10^{-4}$   $\Omega$  cm, predominantly due to a high concentration of intrinsic donor type defects. These donors are compensated during annealing at high temperature in a vacuum; the low resistivity increases and the layers are not thermally stable. At rf power densities of  $\sim 3.2$  W/cm<sup>2</sup> and more, the deposition conditions yield a high growth rate and the extrinsic aluminum dopant is incorporated on vacant cation sites. These substitutional donors are thermally stable therefore a low resistivity is retained after annealing at 550 °C. © 2001 American Vacuum Society. [DOI: 10.1116/1.1329121]

## I. INTRODUCTION

Transparent conducting oxides have attracted much attention in the growing market of flat panel displays and thin film solar cells.<sup>1,2</sup> ZnO is a low cost and abundant material and with a band gap of 3.3 eV it shows an excellent transparency for the entire visible spectrum. Low resistivity and highly transparent layers have been deposited with a variety of deposition methods such as metalorganic chemical vapor deposition,<sup>3</sup> laser ablation,<sup>4</sup> spray pyrolysis,<sup>5</sup> the solgel technique,<sup>6</sup> and sputtering.<sup>7</sup>

The electrical conductivity of ZnO is controlled by intrinsic defects, i.e., oxygen vacancies<sup>8</sup> and/or zinc interstitials,<sup>9</sup> which act as *n*-type donors. The resistivity is lowered further by extrinsic doping with group III elements such as B, Al, Ga, or In.<sup>10</sup> Annealing experiments up to 400 °C showed that the conduction due to intrinsic defects is thermally unstable,<sup>11</sup> whereas a better thermal stability is observed on layers which are doped extrinsically by indium<sup>12</sup> or aluminum.<sup>13</sup>

Thermally stable layers are required for a variety of applications. For example, ZnO:Al layers are used as front contacts in Cu(In,Ga)Se<sub>2</sub> based superstrate solar cells.<sup>14,15</sup> In this configuration, the absorber layer is grown on the transparent ZnO:Al layer at temperatures of about 550 °C. The resistivity of the front contact is expected to change because of annealing of the layer and/or diffusion of impurities. For high efficiency solar cells, it is essential that the resistivity of the front contact remains as low as possible under these conditions. Therefore, we have deposited ZnO:Al layers, annealed them at 550 °C, and correlated the variations of the electrical properties with the growth conditions in order to optimize the thermal stability of ZnO:Al layers. Furthermore, the layers were grown at high rf power to enhance the growth rate which is technologically important.

## II. EXPERIMENT

ZnO:Al layers were grown by rf sputtering in a vacuum chamber with a base pressure of about  $10^{-5}$  Pa. The system is equipped with ceramic sputter targets of pure ZnO and of ZnO mixed with 2 wt% Al<sub>2</sub>O<sub>3</sub> (diameter 100 mm, purity 99.999%). The layers were grown at an argon pressure of 0.3 Pa, except for room temperature depositions, where a partial pressure of 0.5% O<sub>2</sub> in the initial stage is required for the high transparency of the films. The substrate is positioned 40 mm below the targets, it is electrically grounded, and equipped with radiation heating up to substrate temperatures of 400 °C. During the sputtering of layers without intentional heating, the temperature of the substrates is increased to about 60 °C–90 °C, depending on rf power. Samples deposited at high temperature were allowed to cool in a vacuum. We have deposited ZnO:Al layers at rf power densities between 1.3 and 5.1 W/cm<sup>2</sup> and temperatures between room temperature and 400 °C.

The layers were grown on Na-containing float glass which is usually used for the production of thin film solar cells. A few depositions on Na-free glass were performed in order to study the effect of Na-diffusion. For the thickness measurements, small areas were etched with HCl and the step height was measured with a stylus profilometer (Dektak3030). The growth rate varied between 10 and 75 nm per min, depending on rf power density.

The resistivity of all samples was measured immediately after the deposition with a four probe measurement. After that, a part of the samples was used for annealing experiments in vacuum at 550 °C. Other samples were used as substrates for the growth of Cu(In,Ga)Se<sub>2</sub> absorber layers. The observed changes in the resistivity of overgrown and annealed ZnO:Al layers are comparable. Hall mobility and carrier density were investigated at room temperature in a van der Pauw configuration on 1 cm<sup>2</sup> samples with Au contact pads.

<sup>a)</sup>Electronic mail: tiwari@phys.ethz.ch

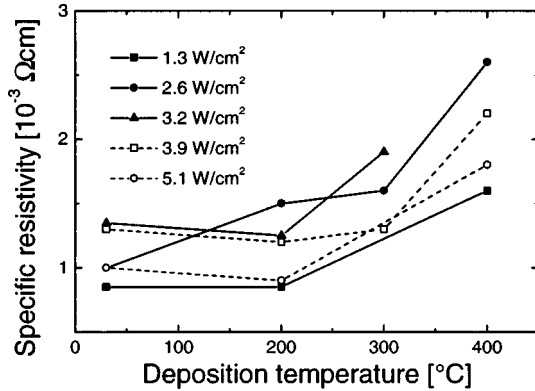


FIG. 1. Dependence of the resistivity on the substrate temperature. Low resistive layers are obtained at deposition temperatures up to 200 °C.

III. RESULTS

A. Electrical properties

Figure 1 shows the dependence of the specific resistivity on the substrate temperature for different rf powers. With the exception of layers deposited at a power density of 2.6 W/cm<sup>2</sup>, there are little differences in the resistivity between depositions at room temperature and 200 °C. A considerable increase in the resistance is observed when the layers are grown above 300 °C.

Figure 2 shows the dependence of the electrical properties on the rf power. Layers with a low resistivity of  $9 \times 10^{-4} \Omega \text{ cm}$  are deposited at low power densities. In the regime of intermediate power density, we observed layers with slightly increased resistivities between 1.3 and 1.5

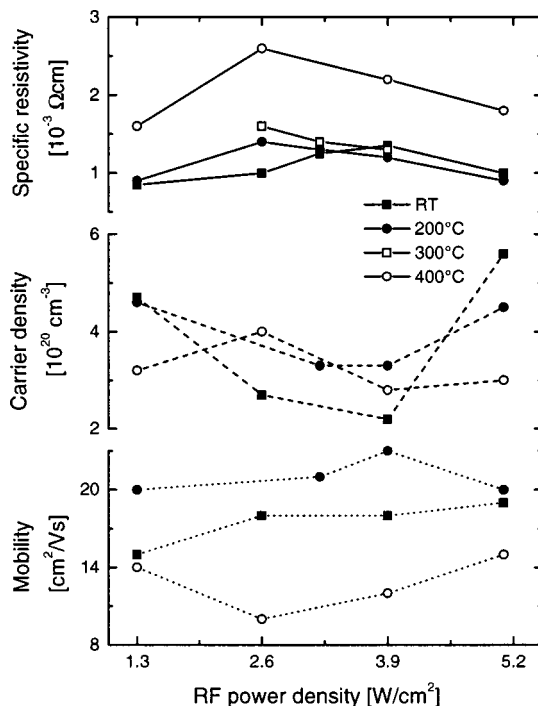


FIG. 2. Dependence of the resistivity, carrier density, and mobility of as-deposited layers on the rf power density.

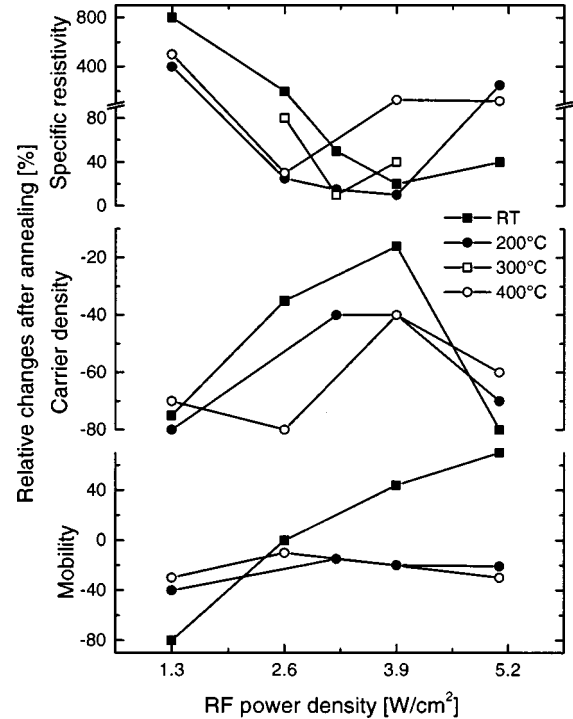


FIG. 3. Relative changes in the electrical parameters after annealing at 550 °C. Layers deposited in an intermediate regime of rf power density exhibit small changes, they are thermally stable.

$\times 10^{-3} \Omega \text{ cm}$ , in agreement with reported data.<sup>16</sup> At still higher power density, another regime for the deposition of low resistive layers ( $9 \times 10^{-4} \Omega \text{ cm}$ ) has been identified. The growth of layers in this regime yields a high deposition rate which is also technologically important for the fabrication of devices.

It is observed that the behavior of the resistivity to a large extent is reflected by the carrier density and only little by the mobility; low resistivity corresponds to high carrier density and vice versa. Small changes in the mobility with varying power density are observed. Films grown at room temperature have mobilities in the range of 15 to 20 cm<sup>2</sup>/V s, layers deposited at 200 °C exhibit the highest mobilities of about 20 cm<sup>2</sup>/V s, whereas low mobility is observed for layers grown at 400 °C (10 to 15 cm<sup>2</sup>/V s).

Figure 3 presents the relative changes of the electrical properties of the ZnO:Al layers after annealing at 550 °C. The rf power density used for the deposition of the layer shows a strong effect on the amount of the changes in the resistivity; in the low power regime, the resistivity is observed to increase up to 800%. In contrast, highly stable layers with increments of less than 20% are observed in the intermediate range of power densities. Annealing of layers deposited in the regime of high power density leads to increments between 40% and 200%. It is observed that the increments of the resistivity are attributable mostly to losses in the carrier density.

The mobility is effected by the annealing only in the case of room temperature deposited layers. At low rf power density, these layers exhibit a loss of more than 80%, whereas

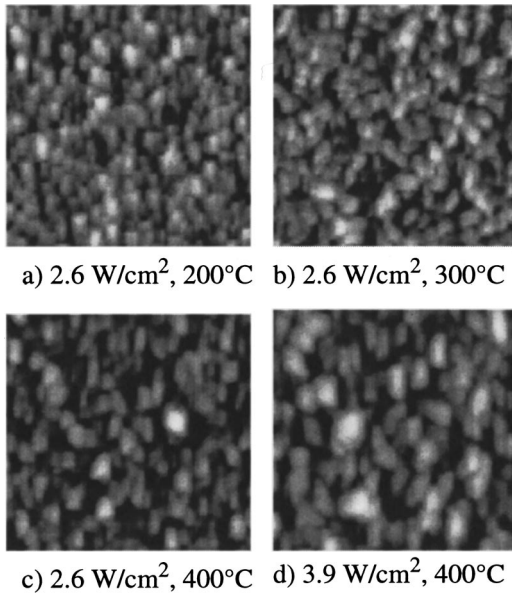


FIG. 4. AFM images show the dependence of the morphology on the deposition parameters (image size  $2 \times 2 \mu\text{m}$ ). The grain size and roughness in (a), (b), and (c) increase with increasing substrate temperature. The images (c) and (d) compare the influence of the power density at the same temperature.

the films grown at high rf power density actually show an increase of the mobility of up to 60%. This increase compensates for the effect of the charge carrier loss which leads to the moderate increase in resistivity of 20%–40% for layers grown at room temperature and high power density. The layers deposited at elevated temperatures do not show this behavior; uniform losses of  $\sim 30\%$  of the mobility are observed.

### B. Structural and morphological properties

The growth rate varies linearly from 10 nm/min at a rf power density of  $1.3 \text{ W/cm}^2$  to 75 nm/min at  $5.1 \text{ W/cm}^2$ . Figure 4 shows atomic force micrograph (AFM) images of layers grown under different conditions. The grain size increases with increasing substrate temperature, but the layers show a higher roughness and they are less compact. An increase of the rf power density shows a similar effect on the grain size and the roughness.

The structural properties were studied by x-ray diffraction (XRD) in  $\theta$ - $2\theta$  configuration. Figure 5 shows diffraction patterns of samples which were deposited at different power densities. It is observed that layers grown at high power density lose their strong preferential texture in the [0002] direction and contributions of the [1010] and [1011] orientations appear.

### C. Influence of sodium

Table I compares the electrical parameters of depositions on Na-free glass and Na-containing float glass. Samples grown at room temperature show no difference, neither in the as-deposited state nor after annealing. If the layer is deposited at high temperature, a lower initial resistivity is mea-

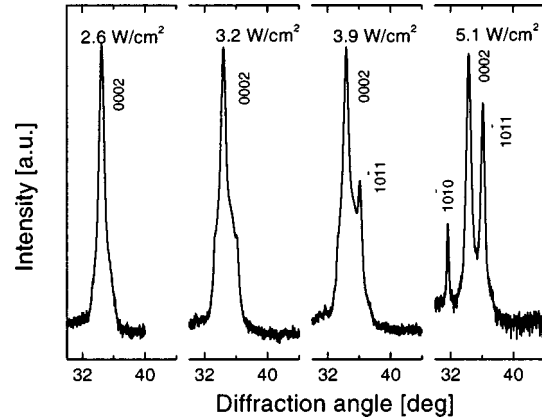


FIG. 5. X-ray diffractograms of ZnO:Al films deposited at different power densities (deposition temperature  $200^\circ\text{C}$ ).

sured on the Na-free glass which is due to higher mobility as well as carrier density. The increase of the resistivity of high temperature grown samples due to annealing is the same for layers on Na-free and Na-containing glass.

## IV. DISCUSSION

The increase of the resistivity with increased substrate temperature above  $200^\circ\text{C}$ , as observed in Fig. 1, has been attributed to a migration of the aluminum dopant towards the grain boundary, where it reacts with adsorbed oxygen and segregates as  $\text{Al}_2\text{O}_3$ . Thus, the potential barrier for charge transport across the grains is increased and a lower mobility results in an increased resistivity as suggested in the literature.<sup>17</sup> Additionally, as observed in Fig. 4, the grain size increases with increasing substrate temperature. The layers show a higher roughness and they are less compact which could also limit the mobility and the charge transport across the grains.

The dependence of the resistivity on the rf power density in Fig. 2 is governed by three regimes. The regimes of low and high rf power density yield layers with low resistivity and Fig. 3 shows that they are not stable against annealing. Layers deposited in the regime of intermediate power density, on the other hand, show a slightly higher initial resistivity but they are highly stable, i.e., their resistivities do not change after annealing at  $550^\circ\text{C}$ .

We believe that this behavior can be explained by an effect of ion bombardment on the formation of donor type intrinsic defects. Impinging ions from the plasma are reported either to damage the growing film<sup>18</sup> or to enhance the surface mobility of adatoms, thereby leading to an improved crystal quality.<sup>19–21</sup> This trade off between the damaging and beneficial effects of the ion bombardment is reflected in the three regimes of resistivity and carrier concentration which is visible in Fig. 2.

At low rf power, only little energy is transferred to the substrate by argon ions. Also, the energy in the plasma is not sufficient for a complete dissociation of  $\text{Al}_2\text{O}_3$ . Sputtered particles move to the substrate and stay at whatever place they arrive; surface diffusion and reorganization is limited. Thus, in the layer, small grains and defects like zinc intersti-

TABLE I. Comparison of the electrical properties and their changes due to annealing at 550 °C. Layers were deposited on Na-free and Na-containing glass at a rf power density of 3.9 W/cm<sup>2</sup>.

Deposition temperature	Substrate	Carrier density (10 <sup>20</sup> cm <sup>-3</sup> )		Mobility (cm <sup>2</sup> /V s)		1/enμ (10 <sup>-3</sup> Ω cm)	
		n <sub>i</sub>	n <sub>f</sub>	μ <sub>i</sub>	μ <sub>f</sub>	ρ <sub>i</sub>	ρ <sub>f</sub>
RT	Float	2.2	1.7	18	23	1.6	1.6
	Na-free	2.1	1.6	19	23	1.6	1.7
400 °C	Float	2.8	1.6	12	10	1.9	3.9
	Na-free	3.4	1.7	17	17	1.1	2.2

tials and oxygen vacancies are formed. The conduction mechanism is governed by a high concentration of donor type intrinsic defects which results in low resistivity. Upon annealing, the donor type defects recombine with oxygen which is desorbed from the grain boundaries which leads to a big increase in the resistivity.<sup>11</sup>

At intermediate powers, a higher flux and higher energies of argon ions provide enough energy for the dissociation of Al<sub>2</sub>O<sub>3</sub> and for the enhancement of surface diffusion of adatoms. Since larger grains with less defects are formed, the conductivity is no longer governed by a high concentration of intrinsic defects but by extrinsic donors (aluminum on the zinc site); thus the resistivity is slightly increased. However, extrinsic donors on substitutional sites show a higher thermal stability than intrinsic donor type defects.<sup>13</sup> Thus, the resistivity increases only marginally upon annealing.

At high powers, the growth rate is high and donor type defects are produced due to impinging ionized species which lower the resistivity. XRD measurements of these layers additionally show that the growth kinetics are changed and a loss in the preferential [0002] texture is accompanied by increasing contributions of grains with other orientations. Annealing of these layers again removes the defect type donors which gives rise to increased resistivity.

The comparison of the electrical parameters of layers on Na-free and Na-containing glass in Table I suggests that sodium is incorporated into the layer only during growth at high temperatures. The samples grown at room temperature exhibit identical behavior on the two kinds of substrates, both in the as-deposited state and after annealing. In contrast, the carrier density of layers deposited at high temperature shows that during growth sodium substitutes on a cation site, forming an acceptor. The change in resistivity of the high temperature grown layers after annealing is again the same on both types of substrates which proves that the increase is not related to Na incorporation into the film.

## V. CONCLUSIONS

The influence of deposition parameters on the electrical properties of ZnO:Al revealed a dependence on the rf power density. Three power regimes are identified which yield layers with different defect behaviors. In the low and high power regions, layers with low resistivity are obtained. However, they are not thermally stable because the conduction is dominated by donor type defects which are compensated

during anneal. A regime of intermediate power density has been identified which, in combination with substrate temperatures between 200 °C and 250 °C, yields thermally stable layers because the conduction mechanism is governed by the aluminum dopant on a zinc site. Layers deposited in this regime are suitable as transparent contacts for applications where process temperatures up to 550 °C are required.

## ACKNOWLEDGMENTS

Dr. Richard Menner (ZSW Stuttgart) and Dr. Ralf Wendt (ANTEC Kelkheim) are thankfully acknowledged for discussions about the sputtering process. The investigations were performed within the Wide-Gap CPV project of the European Joule program and supported by a grant from the Swiss Office of Education and Science.

- <sup>1</sup>K. L. Chopra, S. Major, and D. K. Pandaya, *Thin Solid Films* **102**, 1 (1983).
- <sup>2</sup>H. L. Hartnagel, A. L. Dawar, A. K. Jain, and C. Jagadish, *Semiconducting Transparent Thin Films* (IOP, Bristol, 1995).
- <sup>3</sup>A. Wang, J. Dai, J. Cheng, M. P. Chudzick, T. J. Marks, R. P. H. Chang, and C. R. Kannewurf, *Appl. Phys. Lett.* **73**, 327 (1998).
- <sup>4</sup>H. Kim, C. M. Gilmore, J. S. Horwitz, A. Pique, H. Murata, G. P. Kushto, R. Schlaf, Z. H. Kafafi, and D. B. Chrisley, *Appl. Phys. Lett.* **76**, 259 (2000).
- <sup>5</sup>S. A. Studenikin, N. Golego, and M. Cocivera, *J. Appl. Phys.* **87**, 2413 (2000).
- <sup>6</sup>A. E. Jimenez-Gonzalez, J. A. Soto, and R. Suarez-Parra, *J. Cryst. Growth* **192**, 430 (1998).
- <sup>7</sup>T. Minami, *J. Vac. Sci. Technol. A* **17**, 1765 (1999).
- <sup>8</sup>J. Schoenes, K. Kanazawa, and E. Kay, *J. Appl. Phys.* **48**, 2537 (1977).
- <sup>9</sup>G. Neumann, *Phys. Status Solidi A* **105**, 605 (1981).
- <sup>10</sup>T. Minami, H. Sato, H. Nanto, and S. Takata, *Jpn. J. Appl. Phys., Part 2* **24**, L781 (1985).
- <sup>11</sup>T. Minami, H. Hanato, S. Shooji, and S. Takata, *Thin Solid Films* **111**, 167 (1984).
- <sup>12</sup>S. Major, A. Bannerjee, and K. L. Chopra, *Thin Solid Films* **122**, 31 (1984).
- <sup>13</sup>S. Takata, T. Minami, and H. Nanto, *Thin Solid Films* **135**, 183 (1986).
- <sup>14</sup>T. Nakada, T. Kume, and A. Kunoika, *Sol. Energy Mater. Sol. Cells* **50**, 97 (1998).
- <sup>15</sup>F.-J. Haug, M. Krejci, H. Zogg, A. N. Tiwari, M. Kirsch, and S. Siebentritt, *Thin Solid Films* **361–362**, 239 (2000).
- <sup>16</sup>D. Dimova-Malinovska, N. Tzenov, T. Tzolov, and L. Vassilev, *Mater. Sci. Eng., B* **52**, 59 (1998).
- <sup>17</sup>T. Minami, H. Sato, H. Nanto, and S. Takata, *Thin Solid Films* **171**, 307 (1989).
- <sup>18</sup>K. Tominaga, K. Kuroda, and O. Tada, *Jpn. J. Appl. Phys., Part 1* **27**, 1176 (1988).
- <sup>19</sup>A. Kuroyanagi, *J. Appl. Phys.* **66**, 5492 (1989).
- <sup>20</sup>T. Minami, H. Sato, H. Imamoto, and S. Takata, *Jpn. J. Appl. Phys., Part 2* **31**, L252 (1992).
- <sup>21</sup>R. Cebulla, R. Wendt, and K. Ellmer, *J. Appl. Phys.* **83**, 1087 (1998).